



RESEARCH ARTICLE

The reconstructed evolutionary history of the *Engelhardia spicata* complex highlights the impact of a three-tiered landform in the Indo-Burma ecoregion

Can-Yu Zhang^{1,2} | Guan-Long Cao^{2,3,4,5} | Jian-Lin Hu⁶ | Pei-Han Huang^{2,5} |
Min Li^{2,5} | Ren-Ping Su^{2,5} | Ou-Yan Fang^{2,5} | Xiang Cai^{2,5} | Yi-Gang Song⁷ |
Guo-Xiong Hu⁸ | Kai-Qing Xie⁹ | Lang Li² | Shi-Shun Zhou¹⁰ | Yun-Hong Tan¹⁰ |
Hong-Hu Meng^{2,10}  | Jie Li² 

¹Yunnan Normal University, Kunming, Yunnan 650500, China

²Plant Phylogenetics and Conservation Group, Center for Integrative Conservation, Yunnan Key Laboratory for Conservation of Tropical Rainforests and Asian Elephants, and Yunnan International Joint Laboratory for the Conservation and Utilization of Tropical Timber Tree Species, Xishuangbanna Tropical Botanical Garden, Chinese Academy of Sciences, Kunming 650023, China

³State Key Laboratory of Plant Diversity and Specialty Crops, Institute of Botany, Chinese Academy of Sciences, Beijing 100093, China

⁴China National Botanical Garden, Beijing 100093, China

⁵University of Chinese Academy of Sciences, Beijing 100049, China

⁶Engineering Research Center of Sustainable Development and Utilization of Biomass Energy, Ministry of Education; School of Life Sciences, Yunnan Normal University, Kunming 650500, China

⁷Eastern China Conservation Centre for Wild Endangered Plant Resources, Shanghai Chenshan Botanical Garden, Shanghai 201602, China

⁸College of Life Sciences, Guizhou University, Guiyang 550025, China

⁹College of Agriculture and Biological Science, Dali University, Dali 671003, China

¹⁰Southeast Asia Biodiversity Research Institute, Chinese Academy of Sciences, Myanmar

Correspondence

Can-Yu Zhang, Yunnan Normal University, 768 Juxian Street, Chenggong District, Kunming 650500, Yunnan, China.

Email: zhangcanyu11@outlook.com

Hong-Hu Meng and Jie Li, Plant Phylogenetics and Conservation Group, Center for Integrative Conservation, Yunnan Key Laboratory for Conservation of Tropical Rainforests and Asian Elephants, and Yunnan International Joint Laboratory for the Conservation and Utilization of Tropical Timber Tree Species, Xishuangbanna Tropical Botanical Garden, Chinese Academy of Sciences, 88 Xuefu Road, Wuhua District, Kunming 650023, China.

Email: menghonghu@xtbg.ac.cn and jieli@xtbg.ac.cn

Abstract

Premise: The lateral displacement of the Indochina Peninsula, driven by the Indian–Asian plate collision, significantly altered the topography of the Indo-Burma ecoregion, affecting its climate and biological evolution. Despite the renowned biodiversity of the region, spatiotemporal patterns of evolution remain poorly understood.

Methods: We analyzed the *Engelhardia spicata* complex, which has a continuous distribution across Indo-Burma, based on a robust phylogenetic framework comprising 778 individuals from 80 populations, to elucidate spatiotemporal and paleogeological patterns of evolution. We used ancestral area reconstruction to reconstruct the historical biogeography of the species complex and to understand the broader evolutionary history of the Indo-Burma ecoregion.

Results: An initial divergence within the *E. spicata* complex approximately 26.62 million years ago (Ma) separated a lineage in the Truong Son Mountain Range from one in the Hengduan Mountains and the Shan Plateau. The Shan Plateau and Hengduan Mountain lineages subsequently diverged around 23.03 Ma. These results highlight a three-tiered landform in the Indo-Burma ecoregion, characterized by high-elevation northern regions (Hengduan Mountains, Yunnan-Guizhou Plateau), intermediate-elevation central plateau (Shan Plateau), and low-elevation southern ranges (southern Truong Son Mountains).

Can-Yu Zhang and Guan-Long Cao contributed equally to this work.

Conclusions: Our findings support the tectonic hypothesis that crustal thickening and lateral extrusion of Indochina occurred simultaneously during the Late Oligocene, which led to the formation of the Indo-Burma ecoregion and highlights the biological significance of the resulting three-tiered landform (north-to-south altitudinal gradients) in these regions, providing novel insights into biogeographic patterns in Southeast Asia.

KEYWORDS

biogeographic patterns, *Engelhardia spicata* complex, Indo-Burma ecoregion, Juglandaceae, spatiotemporal history, three-tiered landform

During the Cenozoic era, one of the most significant tectonic events on Earth was the collision between the Eurasian and Indian plates, which led to the formation of the Qinghai-Tibet Plateau (QTP), encompassing the Hengduan Mountains, the plateau platform (including the Pamir Mountains, Karakoram Mountains, Kunlun Mountains, Qaidam Basin, and Qilian Mountains), and the Himalayas (Mao et al., 2021). This collision also caused lateral displacement of the Indochina Peninsula (Yin and Harrison, 2000; Li et al., 2024; Huang et al., 2025). The collision between the Indian and Eurasian tectonic plates and the initial rapid uplift of the QTP are widely accepted to have occurred during the Paleocene (Ding et al., 2022), with subsequent localized uplift during the Oligocene, Miocene and even Pliocene epochs (Luo et al., 2022; Lai et al., 2025a, 2025b). This sustained uplift induced clockwise rotation and southeastward extrusion of the Indochina Peninsula along the Ailao Shan-Red River shear zone, as described by a two-phase acceleration-deceleration model (Liu et al., 2012; Li et al., 2024). This extrusion may also have contributed to the north-high-south-low topographic structure of the Indochina Peninsula. The ongoing extension of the Ailao Shan-Red River shear zone toward southern Vietnam may have played a significant role in shaping the modern Truong Son Mountain Range. During the same period, widespread uplift in the western part of China resulted in high western and low eastern terrain features that have since characterized the region's topography (Che et al., 2010). This geomorphological pattern prompts a critical question: Did similar tectonic processes such as crustal thickening and lateral extrusion similarly shape the adjacent Indo-Burma ecoregion?

The Indo-Burma ecoregion, situated in northern Southeast Asia, is recognized as a distinct bioregion that encompasses the Indochina Peninsula and surrounding areas. The northern boundary of the region is defined by the Eastern Himalayas and subtropical regions (Meng et al., 2025) and the southern boundary by the Isthmus of Kra (Meng and Song, 2023). This biological subregion serves as a crucial link between Eurasia and the Malay Archipelago, facilitating regional biodiversity convergence, diffusion, and migration (Meng and Song, 2023). The tiered topography (i.e., high-elevation northern ranges, intermediate plateaus, and southern lowlands) of the region mirrors the geomorphological gradient in western China. The complex topography of this crucial biogeographic corridor

between Eurasia and the Malay Archipelago has facilitated biodiversity convergence, diffusion, and migration (Meng and Song, 2023). This global biodiversity hotspot (Myers et al., 2000) is home to over 13,500 plant species, of which 7000 are endemic (van Dijk et al., 1999; Mittermeier et al., 2005) and consequently, of significant importance for conserving global biodiversity. The extraordinary biodiversity can be attributed to a combination of complex geological and climatic histories, combined with habitat diversity driven by variations in topography, climate, and latitude (Mittermeier et al., 2002). The intricate geological events since the Paleocene and extending well into the Miocene have profoundly influenced climate and vegetation changes across Southeast Asia (Kooyman et al., 2019), shaping the origin, evolution, and geographical distribution patterns of biodiversity in the region. Understanding the geographic distribution patterns of organisms in the Indo-Burma ecoregion better should enhance biodiversity conservation efforts from evolutionary and ecological perspectives (Woodruff, 2010). Biogeographical studies in the Indo-Burma ecoregion to date have focused primarily on animals, including the families Ichthyophiidae (Gower et al., 2002), Dicroglossidae (Bossuyt and Milinkovitch, 2001; Che et al., 2010), and Ranidae (Wu et al., 2020). Phyto-geographic research has focused on the extrusion of the Indo-Burma ecoregion (Zhao et al., 2016; Meng et al., 2022b; Huang et al., 2023; Li et al., 2024; Zhang et al., 2024). However, the role of topographical dynamics in shaping biogeographic processes across the broader Indo-Burma ecoregion, particularly its elevational gradient from the northern highlands to the southern lowlands, is poorly understood. This elevational gradient parallels the “three-tiered” topography of China (Figure 1), where stepwise geological uplift has profoundly influenced species diversification (Lee, 1939; Clark et al., 2005). Whether similar geomorphological processes shaped the Indo-Burma ecoregion is debated, with limited biological evidence linking extant species distributions to tectonic history (Maneerat and Bürgmann, 2022). We hypothesized that the biogeographic patterns of *Engelhardia* Leschenault ex Blume—a lineage of trees within the Juglandaceae (walnut family) now recognized as a species complex (Manos et al., 2007; Meng et al., 2022b)—potentially mirror the phased uplift of the Indo-Burma terrain. By analyzing the spatial genetic structure in this complex, we aimed to disentangle how Cenozoic geological evolution may have driven diversification in this ecoregion.

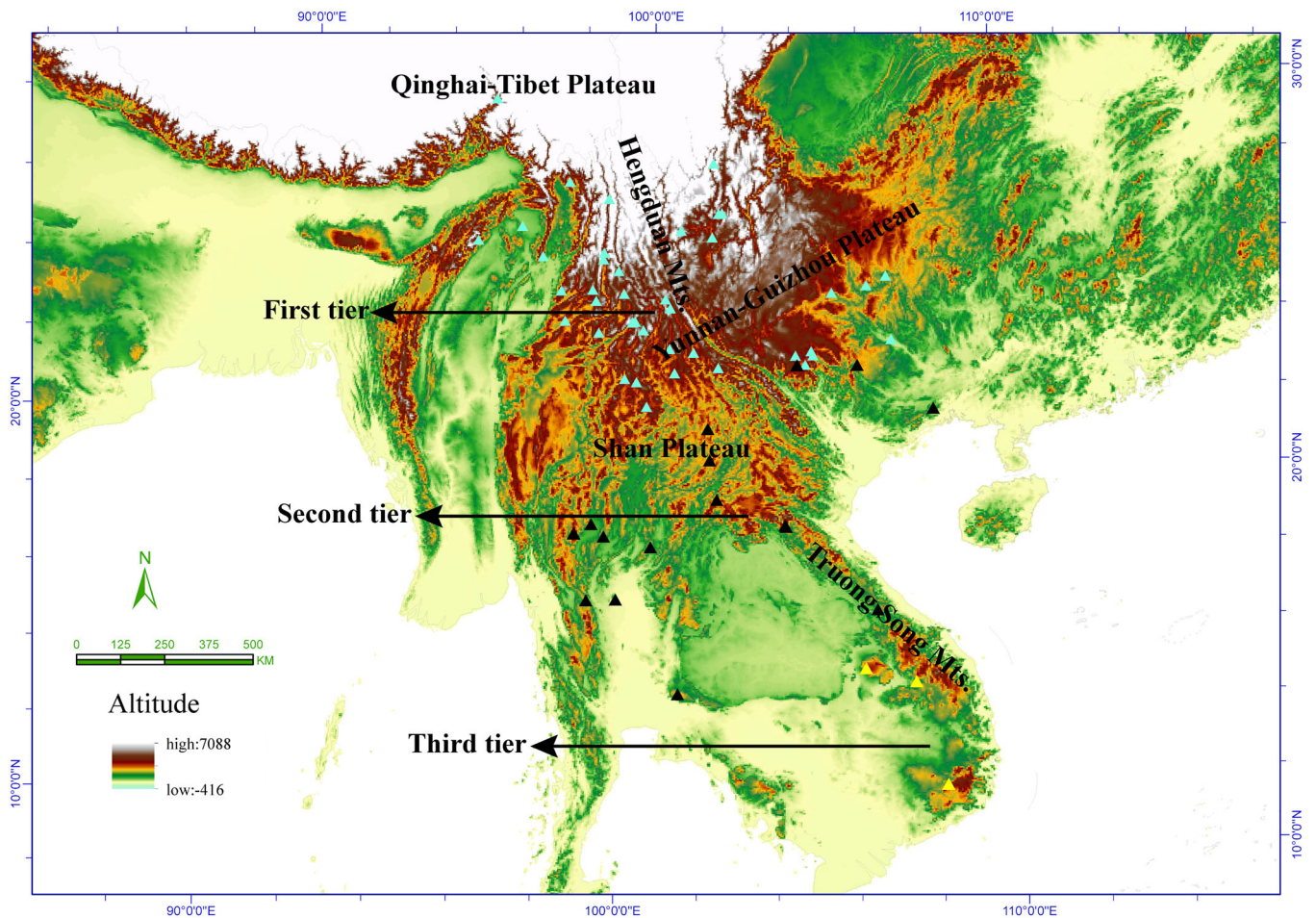


FIGURE 1 Sample distribution and results for plastid DNA sequences. Colored triangles indicate different lineages (blue: group A, black: group B, yellow: group C). The three-tiered landform of the Indo-Burma ecoregion is shown (average elevations a.s.l.: first tier, 4000–5000 m; second tier, 1000–2000 m; third tier, <500 m).

Engelhardia has a long evolutionary history in the region and provides critical insights for reconstructing biogeographic patterns across tropical and subtropical Asia (Song et al., 2020; Huang et al., 2024). Molecular and morphological data indicate that there are nine species in *Engelhardia*, six of which are found in the Indo-Burma ecoregion (Zhang et al., 2020; Meng et al., 2022a). *Engelhardia spicata* is the most widely distributed species. Our previous research demonstrated that the relationship between *E. spicata* and its constituent taxa is complex; the complex includes *E. spicata* var. *aceriflora*, *E. spicata* var. *colebrookeana*, and *E. rigida* (Zhang et al., 2020). The *Engelhardia spicata* complex is primarily distributed in southwestern China (including Tibet, Yunnan, Sichuan, Guangxi, and Guizhou), Myanmar, Thailand, Vietnam, Laos, Indonesia, Malaysia, Nepal, and the Philippines (Zhang et al., 2020). The complex lives at elevations ranging from 142 to 1880 m a.s.l. and is commonly found on slopes within mixed broad-leaf forests or at the forest edges (Appendix S1: Table S1). The distinctive distribution pattern of the complex, spanning diverse topographical

gradients and geological formations provides a valuable model for investigating the impact of geological events in the Indo-Burma ecoregion.

An exploration of spatial and temporal changes in the staircase landform in the Indo-Burma ecoregion should enhance our understanding of causes and mechanisms related to the formation and evolution of this natural environment during the Cenozoic era. Our study addressed two key questions: (1) When did the three-tiered landform of the Indo-Burma ecoregion begin to form and influence distribution patterns of *Engelhardia spicata* complex? (2) How did the geological processes contribute to the formation of the three-tiered landform and to the distribution patterns of *E. spicata* complex in particular? To address these questions, we characterized the phylogeography of the *E. spicata* complex based on alignments of five plastid DNA regions and nuclear ribosomal (nrDNA) data from 80 populations across the Indo-Burma ecoregion, to illuminate the spatiotemporal evolutionary patterns of plants in the Indo-Burma ecoregion and investigate the topographic structure of the region from a biological perspective.

MATERIALS AND METHODS

Sample collection and DNA analysis

We collected a total of 778 individuals of the *E. spicata* complex from 80 populations across the Indo-Burma ecoregion (Figure 2; Appendix S1: Table S1). The sampling locations span the Indo-Burma ecoregion and parts of southern China and encompass a diverse range of topographical gradients and geological formations. We obtained meta-data relevant to these areas from various published (Manning, 1966; *Flora of China*, Lu et al., 1999) and online sources (Chinese Virtual Herbarium [CVH; <https://www.cvh.ac.cn>]; Global Biodiversity Information Facility [GBIF; <https://www.gbif.org>]). We extracted total genomic DNA for these samples using a Plant Genomic DNA Kit (Tiangen Biotech, Beijing, China). We recovered five plastid DNA regions (*psbA-trnH*, *trnL-trnF*, *rps16*, *trnS-trnG*, and *rpl32-trnL*) based on laboratory protocols detailed in Appendix S1: Table S2. We concatenated the five plastid fragments using Geneious v6.1.2 (<https://www.geneious.com/>). We then used

DnaSP v6 (Rozas et al., 2017) to identify and determine haplotypes and ITS genotypes. Table S1 in Appendix S1 details the number and distribution of different haplotypes and ribotypes across populations. We determined haplotype diversity (H_d) and the selective neutrality parameters Tajima's D (Tajima, 1989) and Fu and Li's D^* (Fu and Li, 1993; Fu, 1997) using DnaSP v6 for the combined plastid DNA haplotype (H) and ITS ribotype (R). And employed Arlequin v3.1 (Excoffier et al., 2007) for an analysis of molecular variance (AMOVA) (Excoffier et al., 1992) using both the concatenated plastid DNA sequences and ITS data. We assessed genetic variation within and among populations using Φ - and R -statistics. We assessed the significance of fixation indices using 1000 permutations and tested a null hypothesis of spatial expansion using mismatch distribution analysis (MDA) in DnaSP v6. We assessed the goodness-of-fit of population demographic history by calculating the sum of squared deviations between the observed and expected mismatch distributions and the raggedness index (HRag). These calculations were based on 1000 parametric bootstrap replicates (Harpending, 1994).

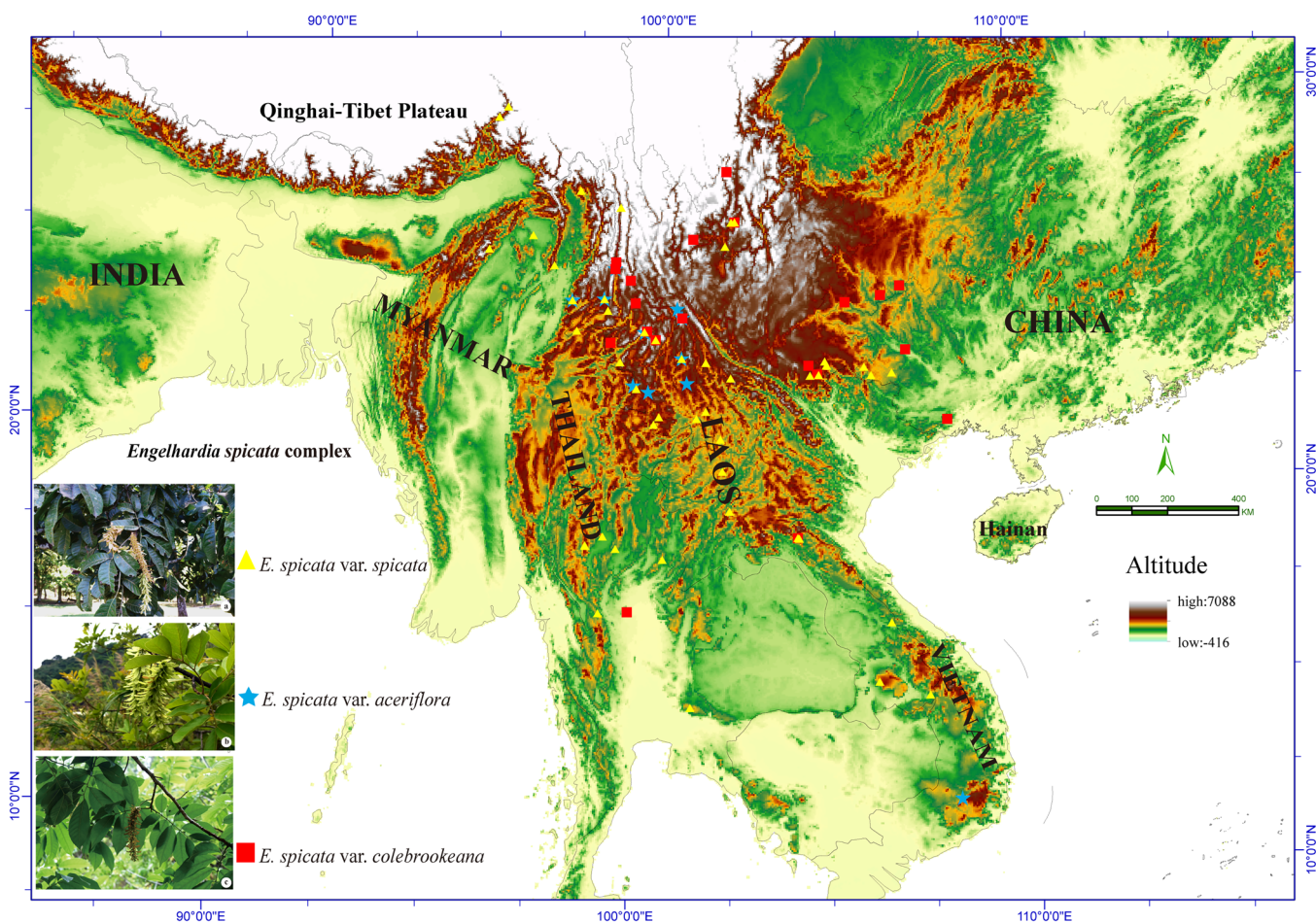


FIGURE 2 Geographic distribution of the *Engelhardia spicata* complex across the Indo-Burma ecoregion and parts of southern China. A total of 80 locations were studied across. Sample localities: red triangles, *E. spicata* var. *spicata*; black stars, *E. spicata* var. *aceriflora*; blue squares, *E. spicata* var. *colebrookeana*.

DNA sequence phylogenetic analyses

We inferred the lineage relationships between *H* and *R* from a median-joining network using NETWORK v2.0 (Bandelt et al., 1999). Separately, based on previous phylogenetic inferences in Juglandaceae (Manos and Stone, 2001; Manos et al., 2007; Zhang et al., 2020; Meng et al., 2022a), we selected *Engelhardia fenzelii*, *E. roxburghiana*, *E. hainanensis*, *E. villosa*, *E. serrata*, *E. apoensis*, and *Rhoiptelea chiliantha* as outgroups. We inferred phylogenies using Bayesian inference for the plastid DNA and ITS data sets with MrBayes v3.1.2 (Huelsenbeck and Ronquist, 2001). We determined the best-fit DNA substitution model for each data set using the Akaike information criterion (AIC) and PAUP* version 4.0b10 (Swofford, 2002) and MrModeltest 2.4 (Nylander, 2004). The optimal substitution models proposed for the combined plastid DNA and nrDNA data were GTR + I + G and GTR + G, respectively. For the Bayesian analyses, we ran the MCMC algorithm for 5×10^6 generations, using a cold chain and three heated chains, starting from random trees, sampling every 5000 generations and discarding the first 10% as burn-in. All effective sample size (ESS) values were >200. We also used IQ-TREE v2.1.1 (Minh et al., 2020) for maximum likelihood (ML) analyses, including a model selection analysis for each data set. To identify the best ML tree, we ran five independent analyses, each searching for the optimal tree topology. Subsequently, we ran a single analysis with 1000 ultrafast bootstrap replicates (Minh et al., 2020).

Divergence time estimation

To avoid potential biases due to recombination and incomplete concerted evolution in nuclear sequences on age estimates (Álvarez and Wendel, 2003; Emadzade and Hörandl, 2011), we used the plastid data rather than the combined plastid and nuclear data. For comparative purposes, we also estimated divergence times using the ITS data set. We analyzed these data sets using BEAST v1.8.1, which implements the Bayesian MCMC algorithm for phylogenetic inference and molecular dating (Drummond and Rambaut, 2007). For these analyses, we used nucleotide substitution models identical to those described for the Bayesian phylogenetic analysis above. We compared four clock models (strict, uncorrelated relaxed, random, and fixed) and two tree speciation priors (Yule and birth–death) using Bayes factors (Kass and Raftery, 1995) calculated from marginal likelihoods derived from path sampling (Baele et al., 2013). The uncorrelated relaxed clock model (Appendix S1: Table S3) and Yule tree prior model (Appendix S1: Table S4) were identified as the best-fit models. For the uncorrelated relaxed clock model, we used a normal distribution to define the prior for the mean substitution rate parameter, and for the GTR + G model for each DNA region separately, we considered mean values for parameters of the distribution (Ho and Phillips, 2009). For

the MCMC analysis, we set the combined plastid DNA and ITS chain length to 3×10^8 generations, sampling every 10,000 generations. All options were configured using BEAUTi v1.8.1 in BEAST.

We assessed convergence in Tracer v1.6 (Rambaut et al., 2014), and all ESS values were >200. After discarding the first 10% sampled trees as burn-in, we generated a maximum clade credibility (MCC) tree with median ages and 95% highest posterior density (HPD) intervals on nodes using TreeAnnotator v1.8.1 (Drummond and Rambaut, 2007), which we visualized using FigTree v1.4.4 (Rambaut, 2018). Based on phylogenetic analyses of both extant and extinct Engelhardioideae (Meng et al., 2015), we calibrated the dated tree using fossil records of *Alatonucula ignis* (Hermesen and Gandolfo, 2016) and *Paleooreomunnea stoneana* (Dilcher et al., 1976). Specifically, we used (1) *Alatonucula ignis*, the most reliable and oldest known fruit fossil record, found in South America during the Eocene (Hermesen and Gandolfo, 2016) with its $^{40}\text{Ar}/^{39}\text{Ar}$ age = 52.22 ± 0.22 Ma (Wilf, 2012; Barreda et al., 2020), to calibrate the stem group age of Engelhardioideae; (2) *Paleooreomunnea stoneana*, discovered in North America during the Eocene with an estimated age of 40.4–48.6 Ma, to calibrate the Engelhardioideae crown group (Dilcher et al., 1976; Sauquet et al., 2012; Zhang et al., 2013).

Ancestral range reconstruction and elevation analysis

We inferred ancestral distribution ranges of *E. spicata* complex using the R package BioGeoBEARS version (Matzke, 2013), along with plastid DNA fossil-calibrated tree data sets. Based on the weighted AIC corrected for sample size (AICc_{wt}), we compared six biogeographical models: DEC, DEC+j, DIVALIKE, DIVALIKE+j, BAYAREALIKE, and BAYAREALIKE+j. The DEC model was determined to be optimal, exhibiting the highest AICc_{wt} (Appendix S1: Table S5), and was thus used for ancestral area reconstruction. To account for phylogenetic uncertainties, we conducted ancestral range reconstruction using the statistical DEC model as implemented in RASP v4.2 (Ree and Smith, 2008; Yu et al., 2015). We loaded the MCC tree and 1000 randomly selected trees (including outgroups) from the BEAST analysis as input files. Based on the geographic divisions of Wen (2017), we defined four geographic areas: (A) the Hengduan Mountains and the Yunnan-Guizhou Plateau, (B) the Shan Plateau region, (C) the southern Truong Son Mountain Range, (D) all other regions except A, B, and C. Additionally, we generated 50 biogeographic stochastic maps in BioGeoBEARS (Matzke, 2013) to evaluate uncertainty in ancestral range estimation and biome transition dynamics (Appendix S1: Table S6).

In total, we collected data for 187 occurrences of *E. spicata* complex sites from GBIF, CVH, and new field records (Appendix S1: Table S7), excluding localities with

inaccurate or missing coordinates. For each record, we extracted the elevational variable from the calibration dataset for global land areas at 1-km resolution (Fick and Hijmans, 2017) using the function `raster` in the R package `raster` (Hijmans, 2020). We calculated the mean and boundaries of the 95% elevational range for each species. After confirming normality and homogeneity of variances, we used an ANOVA to assess interspecific differences in elevation ranges. IBM SPSS Statistics v22.0 (IBM, Armonk, NY, USA) was used for all calculations and box plots. A squared-change parsimony method is appropriate for analyzing continuous characters (Paradis et al., 2004), and so we inferred the ancestral elevation of the *E. spicata* complex with this method in Mesquite 3.61 (Maddison, 2019), using the MCC tree, with vertical lines of different colors representing the three genetic clusters. For comparative purposes, we also inferred the ancestral elevation using the phylogenetic independent contrast (PIC) method, a Brownian-motion based estimator. We conducted the PIC analysis using the function `ace` in the R package `ape` (Paradis et al., 2004). We also employed the phylogenetic generalized least squares (PGLS) method to analyze the ancestral elevation of the *E. spicata* complex because this method incorporates phylogenetic relationships to account for evolutionary relatedness among species (Grafen, 1989; Martins and Hansen, 1997).

RESULTS

Genetic diversity of plastid DNA and nrDNA

We sequenced a total of 778 samples from the *E. spicata* complex, yielding 724 plastid DNA sequences and 674 ITS sequences. The concatenated alignment of five plastid DNA spacers spans 4647 bp, revealing 51 haplotypes across all samples. The ITS consisted of 755 bp, leading to the identification of 31 ribotypes (Appendix S1: Table S1). We observed high levels of haplotype diversity ($H_d = 0.9664$) and ribotype diversity ($H_d = 0.8675$) across all regions. However, the subregional plastid DNA and ITS diversity values were lower than the overall diversity for all regions, and group A had higher diversity than groups B and C. We summarize the basic genetic data for all species across the major regions in Appendix S1 (Table S1). Variation in plastid haplotype and nuclear ribotypes within populations was greater than reported for *E. roxburghiana* and *E. fenzelii* (within the same genus) (Meng et al., 2022b): populations Y02, M02, Y03, Y05, Y35, Y43, L09, L13, L14, L15, A02, A03, A05, Y10, Y12, and Y18 each had two haplotypes present (the three-letter population codes for each population are defined in Appendix S1: Table S1). Populations M02, Y31, Y34, Y35, Y38, Y41, S08, Y42, L13, A02, A03, Y10, Y12, Y48, and Y49 each had two ribotypes (Appendix S1: Table S1). Most populations were fixed for a single plastid haplotype or nuclear ribotype (see the three-letter codes with an “H” or “R” prefix, respectively, Appendix S1: Table S1),

and some common haplotypes and ribotypes are shared among different populations, for example, plastid haplotypes H01, H02, H05, H06, H11, H15, H16, H17, H19, H20, H23, H25, H26, H29, H34, H37, and H44, and nuclear ribotypes R01, R02, R03, R04, R08, R10, R12, and R23 (Appendix S1: Table S1). The AMOVA based on plastid DNA haplotypes revealed significant and extensive genetic population differentiation ($\Phi_{ST} = 0.91862$, $P < 0.001$), with 49.86% of the genetic variation partitioned among the three regions and 41.99% among populations within those regions (Appendix S1: Table S8). The ITS ribotype Φ_{ST} value was 0.90452 ($P < 0.001$), with 31.80% of the genetic variation partitioned and 58.65% among populations within the regions. The estimates of Tajima's D and Fu's F_S are significant for all plastid DNA clades and subclades of the *E. spicata* complex (Appendix S1: Table S9). The observed mismatch distributions of plastid DNA for each clade/subclade were multimodal and/or highly ragged (Appendix S1: Figure S1), leading to rejection of the spatial expansion model in most cases.

Phylogenetic relationships

The ML tree of plastid DNA haplotypes revealed three distinct lineages, consistent with both BI trees (Appendix S1: Figure S2). Group A comprised populations from the Yunnan-Guizhou Plateau (China) and northern Myanmar, distributed primarily in the high-altitude Hengduan Mountains. Group B included populations predominantly located in the Shan Plateau and adjacent areas of Thailand, Laos, Vietnam, and parts of southern China. Group C comprised populations from the southern section of the Truong Son Mountain Range. The distribution of the plastid DNA phylogeographic structure exhibited a three-tiered geographic genetic pattern, characterized by high-elevation northern regions (the Hengduan Mountains and the Yunnan-Guizhou Plateau), intermediate-elevation central plateaus (the Shan Plateau), and low-elevation southern ranges (the southern Truong Son Mountain Range) (Figure 1). In contrast, nuclear ribotypes had no clear phylogeographic structure (Appendix S1: Figure S3).

Divergence time estimation

Divergence time estimation suggests that *E. fenzelii* and *E. roxburghiana* diverged from their sister lineage within *Engelhardia* by 45.06 Ma (plastid DNA; node ii, 95% HPD: 41.09–49.18 Ma; Table 1; Figures 3B) or 44.82 Ma (ITS; node ii, 95% HPD: 40.84–48.95 Ma; Table 1; Appendix S1: Figure S4). The *E. spicata* complex diverged from its sister lineage, *E. hainanensis* approximately 32.16 Ma (plastid DNA; node iii, 95% HPD: 22–41.97 Ma; Table 1; Figure 3B). The stem age of *E. spicata* group C was around 26.62 Ma (plastid DNA; node iv, 95% HPD: 17.24–36.23 Ma; Table 1;

TABLE 1 Median age and 95% highest posterior density (HPD) estimates in million year ago (Ma) for selected nodes based on plastid DNA and ITS.

Node	Median age (HPD), Ma	
	Plastid DNA	ITS
(i) *Fossil calibration point	52.22 (52.01–52.43)	52.22 (52–52.43)
(ii) *Fossil calibration point	45.06 (41.09–49.18)	44.82 (40.84–48.95)
(iii)	32.16 (22–41.97)	
(iv)	26.62 (17.24–36.23)	
(v)	23.03 (14.79–32.34)	
(vi)	18.13 (10.72–26.92)	
(vii)	15.5 (7.44–25.14)	
(viii)	10.78 (1.13–23.78)	

Figure 3C). The stem age of group A and group B was 23.03 Ma (plastid DNA; node v, 95% HPD: 14.79–32.34 Ma; Table 1; Figure 3C). In contrast, ITS failed to resolve intraspecific divergence events within the *E. spicata* complex, possibly due to incomplete lineage sorting or gene flow. Divergence timelines for major clades based on the plastid data are summarized in Figure 3C and Table 1.

Ancestral range reconstructions

Our ancestral range reconstruction suggests that the most recent common ancestor of the *E. spicata* complex occupied the Indo-Burma ecoregion (node iv; Figure 3B). Within the *E. spicata* complex, two vicariance events occurred (Figure 3C). One led to the divergence of group C in the southern Truong Son Mountain Range, and the most recent common ancestor of group A and group B (node v; Figure 3C). Another vicariance event separated group B in the Shan Plateau region from group A in the Hengduan Mountains and the Yunnan-Guizhou Plateau. Results from the two analytical approaches (BioGeoBEARS and RASP) had strong congruence, supporting the robustness of our reconstructions (Appendix S1: Figure S5). The BioGeoBEARS stochastic mappings (DEC model; 50 replicates) indicated 108.1 ± 1.5 geographic range shifts. Of these, 69 ± 0 were cladogenetic (branching) events compared to 39.1 ± 1.45 anagenetic (within a single branch) dispersal events. Of the 69 branching events, in 52.96 ± 1.32 events, sister species maintained their ancestral biome (“narrow sympatry”), and in 9.96 ± 1.65 events, one sister species maintained its ancestral biome while the other sister occupied only a subset of the ancestral range (“subset sympatry”). The remaining branching events were made up of 6.08 ± 1.1 vicariance events in which the sister species split their ancestral range. Group C in the southern Truong Son

Mountain Range represented the largest source of outward dispersal (11.78 ± 5.7 events), followed by group A in the Hengduan Mountains and the Yunnan-Guizhou Plateau (10.32 ± 5.48 events; Figure 3D). In contrast, the largest sink for inward dispersals was group B in the Shan Plateau region (10.86 ± 4.82 events). The most significant directional transition occurred from group C to group B (4.72 ± 1.87 events; Figure 3D and Appendix S1: Table S6). Furthermore, network analysis of plastid DNA supported three major lineages of the *E. spicata* complex (Appendix S1: Figure S6). The network highlighted the complex genetic relationships between the haplotypes from the southern Truong Son Mountain Range (group C) and those from the other two clades, suggesting potential gene flow and incomplete lineage sorting within this group (Zhang et al., 2020).

Elevation differentiation

The altitude of the study area ranged from approximately sea level to 5000 m a.s.l. and had a stepped distribution (Figure 4A, B). The ancestral elevation reconstructions using the PIC and PGLS methods yielded highly consistent results (Appendix S1: Figure S7). We focus on the PIC results here. The *E. spicata* complex occurs at various elevations, categorized into group A (1351.66 m; 95% HPD: 1289.30–1414.03), group B (1048.65 m; 95% HPD: 880.75–1216.56) and group C (786.88 m; 95% HPD: 650.52–923.25). A variance homogeneity test indicated comparable within-group dispersion ($P > 0.05$), but the Kruskal–Wallis analysis revealed strong elevational differentiation among groups ($P < 0.05$). The strong elevational differentiation among groups ($P < 0.05$) suggests that altitude differentiation among the *E. spicata* complex was significant (Appendix S1: Table S10). Additionally, the reconstruction analysis of ancestral elevation demonstrated that the altitudes of the three groups also exhibited significant elevational differentiation (Figure 4D), i.e., group A at a mean altitude of 1291.6 m (95% HPD: 1281.86–1301.34), group B 1050.03 m (95% HPD: 1041.62–1058.44), and group C 763.5 m (95% HPD: 754.4–772.6).

DISCUSSION

Spatiotemporal evolution of *E. spicata* complex

Tectonic events have profoundly influenced biodiversity and geographical distribution patterns in the Indo-Burma ecoregion (Janssens et al., 2016; Herrera et al., 2021). Furthermore, the evolutionary diversification of organisms may mirror geological and climatic changes (Che et al., 2010; Xiang et al., 2021; Zhang et al., 2023; Zhang et al., 2025). Our molecular dating and geological analyses here not only offer a novel horizon to understanding the evolution of the *E. spicata* complex, but also provide broader insights into the historical biogeography reconstruction of the Indo-Burma ecoregion.

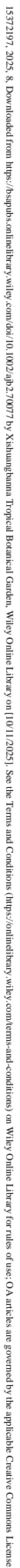


FIGURE 3 Combined chronogram of divergence times from plastid DNA, ancestral area reconstructions, and geological events in the Indo-Burma ecoregion and parts of southern China. (Panel A) Map showing major floristic divisions A–C in the Indo-Burma ecoregion and parts of southern China according to the geographical divisions of Wen (2017), and the related phylogenetic reconstruction in our study: (A) the Hengduan Mountains and the Yunnan-Guizhou Plateau; (B) the Shan Plateau region; (C) the southern Truong Son Mountain Range. (Panel B) Divergence time estimates for all *Engelhardia* species. (Panel C) Ancestral area reconstructions of the *Engelhardia spicata* complex. (Panel D) Bar plot showing the frequency and composition of outward and inward transitions. Colors correspond to different source or sink regions, consistent with panel C.

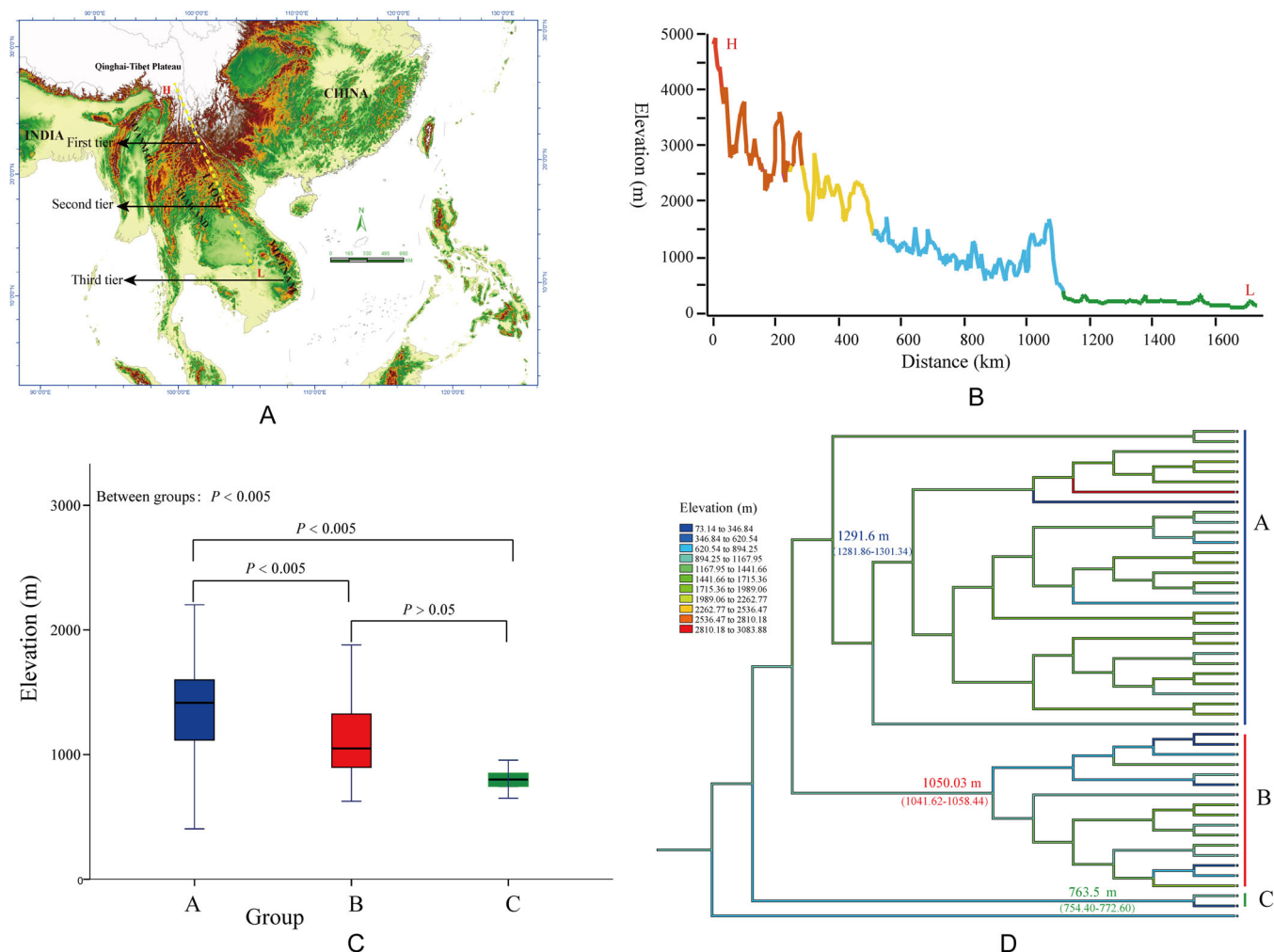


FIGURE 4 The three-tiered altitudinal landform structures of the Indo-Burma ecoregion and elevation differentiation of the *Engelhardia spicata* complex. (Panel A) Depiction of the ecoregion's three-tiered landform, as described in Figure 1. Dotted yellow lines indicate elevation. (Panel B) Modern topographic profile along the transect H-L shown in Panel A. (Panel C) Box and whisker plot indicating the current elevational range for each genetic group of the *Engelhardia spicata* complex. The differences between groups A and B and between groups A and C were statistically significant ($P < 0.05$); groups B and C did not differ significantly ($P > 0.05$) (Appendix S1: Table S10). (Panel D) Ancestral reconstruction of the mean and boundaries of the 95% elevational range using Mesquite 3.61 (Maddison and Maddison, 2019). The branch color represents elevation. Numbers above the branches are the mean and boundaries of the 95% elevational range (m a.s.l.) for ancestral nodes.

Our results indicate that the *E. spicata* complex diverged from its sister lineage, *E. hainanensis* around 32.16 Ma (95% HPD: 22–41.97; Figure 3B, Table 1), which aligns with previous studies that estimated this divergence at ~37.86 Ma (Meng et al., 2022b). This finding may reflect a lateral shift in the Indo-Burma ecoregion, potentially initiated by a significant collision estimated at 30 ± 5 Ma (Wang, 2017). Molecular studies of other lineages have produced similar results, such as the divergence of *Roscoea* (Zingiberaceae) from *Cautleya* (Zingiberaceae) at approximately 32 Ma (Zhao et al., 2016), and the isolation of the central Vietnam lineage of *Stedocys* (Araneae, Scytodidae) from the northern Vietnam and southwestern China lineages at approximately 30 Ma (Luo and Li, 2018). In addition, geological studies report that the left-lateral extrusion of Indochina began at approximately 35 Ma (Schärer et al., 1994; Leloup et al., 2001; Li et al., 2020) and was driven by significant

lithospheric delamination in the Ailao Shan-Red River shear zone (Feng et al., 2021). We propose that the lateral displacement of the Indo-Burma ecoregion occurred as early as the Early Oligocene, with a divergence time estimate of approximately 32.16 Ma. Our integrated results of molecular dating, ancestral range reconstruction, and biogeographic stochastic mapping (BSM) analyses (Figure 3) indicate that the ancestor of the *E. spicata* complex was distributed in the low-elevation region, with subsequent vicariance and dispersal events shaping its current distribution pattern.

The earliest lineages of the complex diverged in the lower-elevation southern region of the Truong Son Mountain Range, marking the initial stage of its diversification. The split between group C and its northern Asian sister group at 26.62 Ma coincides with major patterns of genetic structure within the *E. spicata* complex in the Truong Son Mountain

Range between northern and southern populations (Figure 3C, Table 1). This divergence may reflect far-field effects of the India–Eurasia collision. By the Late Oligocene, the continuous uplift of the QTP, along with the ongoing extension of the Ailao Shan–Red River shear zone (Che et al., 2010) shaped the modern Truong Son Mountain Range, whose complex topography has acted as a barrier to gene flow. The BSM analysis revealed group C as the primary source of outward dispersal (11.78 events), reflecting the ecological connectivity of the Truong Son Mountain Range during the Oligocene. However, subsequent tectonic uplift led to habitat fragmentation, restricting population connectivity. Similar patterns were observed for sympatric species such as *Engelhardia roxburghiana* and *E. fenzlii* (Meng et al., 2022b) and the spiny frog clade (Paini tribe; Che et al., 2010).

Molecular dating revealed the divergence of group A in the Hengduan Mountains and the Yunnan–Guizhou Plateau, and group B in the Shan Plateau, to be around 23.03 Ma (Figure 3C, Table 1). This timing is consistent with significant splits observed in alpine ginger lineages, which are estimated to have occurred approximately 23 Ma (Zhao et al., 2016). It also corresponds to the Oligocene–Miocene boundary (~23 Ma), as suggested by studies on spiny frogs (Che et al., 2010). This time point is generally considered to coincide with a major phase of the ongoing India–Asia collision, which caused the southeastward displacement of Indochina relative to South China along the Ailao Shan–Red River shear zone (Zhao et al., 2016). Geological evidence further supports this scenario, with peak rock metamorphism in the eastern Himalayan syntaxis 23 Ma (Zhang et al., 2012), suggesting that the Asian lithosphere underwent significant alteration around the Oligocene–Miocene boundary. The BSM analysis revealed distinct dispersal patterns among the major clades of *E. spicata*. Group A in the Hengduan Mountains and the Yunnan–Guizhou Plateau was a significant source of outward dispersal, with a total of 10.32 events recorded, reflecting its diverse habitats and historical connectivity. In contrast, group B in the Shan Plateau region was the largest sink for inward dispersals (10.86 events), likely due to its geographic connectivity.

Our findings highlight the interplay between geological events, ecological isolation, and dispersal dynamics in shaping the distribution and genetic structure of the *E. spicata* complex. The simultaneous uplift, strike-slip extrusion, and climatic fluctuations during the Oligocene likely created the conditions necessary to explain the observed patterns of vicariance and dispersal in the complex.

Spatial distribution of genetic diversity and the three-tiered landform pattern

The multimodal and ragged distribution generally indicate that the populations examined here are stable (Appendix S1: Figure S1). The wind-pollinated species has limited long-distance dispersal abilities (Hedrén and Lorenz, 2019;

Kotlínek et al., 2020; da Silva and Abrahão, 2021). This limitation, combined with the rapid uplift of the region, further supports the hypothesis that passive uplift is a primary driver of the elevation distribution of the species complex of *E. spicata*. Consequently, the likely stable populations and their distribution within the Indo-Burma ecoregion make the *E. spicata* complex a valuable model for studying geological evolution and terrain structure in this region.

The *Engelhardia spicata* complex exhibits a pronounced phylogeographic structure. Specifically, the initial divergence between the North Asian group, namely clades A and B and its sister group C, occurred at about 26.62 Ma; subsequently, the split between clades A and B took place around 23.03 Ma. The most recent common ancestor of group A is believed to have emerged in the Hengduan Mountains and Yunnan–Guizhou Plateau approximately 18.13 Ma. The estimated ancestral elevation of group A is approximately 1291.6 m (95% HPD: 1281.86–1301.34), closely corresponding to its current distribution altitude of about 1351.66 m (95% HPD: 1289.3–1414.03) (Figure 4; Appendix S1: Table S10). These findings suggest that the Hengduan Mountains and the Yunnan–Guizhou Plateau had already reached an altitude similar to present-day levels by the early Miocene, establishing the first tier of a three-tiered landform structure. The most recent common ancestor of group B traces back to the Shan Plateau region around 15.5 Ma. The estimated ancestral elevation of group B is about 1050.03 m (95% HPD: 1041.62–1058.44), closely aligning with its current distribution altitude of about 1048.65 m (95% HPD: 880.75–1216.56) (Figure 4; Appendix S1: Table S10). The close alignment between the ancestral (1050.03 m) and current (1048.65 m) elevations indicates that the Shan Plateau achieved an altitude comparable to the present-day levels by the middle Miocene, thus forming the second tier of the landform structure. Furthermore, the most recent common ancestor of group C is thought to have appeared in the southern Truong Son Mountain Range around 10.78 Ma. The estimated ancestral elevation of group C is approximately 763.5 m (95% HPD: 754.4–772.6), which is close to its current distribution altitude of about 786.88 m (95% HPD: 650.52–923.25) (Figure 4; Appendix S1: Table S10). The congruence between ancestral (763.5 m) and contemporary (786.88 m) elevation estimates suggests that the southern Truong Son Mountain Range reached an altitude similar to its present-day levels by the late Miocene, establishing the third tier of the landform structure. Thus, our research supports that the three-tiered landform structure in mainland Southeast Asia had already formed by at least the late Miocene, coinciding with significant geological and climatic changes in the region. This preliminary finding supports the idea that the unique topography of the Indo-Burma ecoregion played a crucial role in shaping its rich biodiversity. However, these conclusions are based on our analysis of limited genetic markers and geological data from one species complex, and so further research is imperative to fully understand the timing and mechanisms

of the formation of the three-tiered landform structure. Future studies incorporating ecological data, such as historical climate records, habitat maps, and species interaction models, will be essential for unraveling the complex interplay between geological events, ecological dynamics, and the evolutionary history of the *E. spicata* complex and of other co-existing lineages.

Terrain refers to the undulating shape of the land resulting from the combined action of internal and external forces acting on Earth. This shape reflects the internal structure, tectonics, composition, and development of the crust at the surface (Zhang et al., 2014). Palaeo-altimetric studies generally agree that substantial surface uplift occurred in eastern Tibet at least 20 Ma before the onset of deep river incision (Ding et al., 2022). The southeastern margin of the QTP experienced significant crustal uplift during the Cenozoic era, with paleoelevation data from various periods indicating differences in the rates and magnitudes of uplift across different regions and time frames (van Hinsbergen et al., 2012; Ding et al., 2022; Lai et al., 2025a, b). Considerable evidence, including structural deformation, sedimentation, and thermal chronology, suggests that orogenic events during the Oligocene were widespread, extending beyond the southern margin of the plateau in the Himalayas and Gangdese Mountains to include the marginal areas of the plateau. These orogenic events resulted in the uplift of the Himalayas, Gangdese Mountains, Longmen Mountains, Tianshan, Ailao Mountains, and East Kunlun Mountains (Wang, 2017). Based on the analysis presented in the previous sentences and the findings of this study, it can be inferred that geological evolution since the Late Oligocene, along with tectonic movements and interactions among the Eurasian, Pacific, and Indian plates in the Indo-Burma ecoregion, were the primary drivers of the north-high-south-low terrain (Fanget et al., 2020; Garcés et al., 2020), and the three-tiered landform. These geological events likely triggered climate change, which in turn led to biotic reorganization across Asia (Meng and Song, 2023). This perspective aligns with the insights of Che et al. (2010), who attributed the emergence of elevated northern terrain and lower southern regions in the Himalayas and QTP to uplift processes that began in the late Oligocene. Similarly, Ding et al. (2022) proposed that the topographically induced flow of a weak lower crust played a crucial role in uplifting the eastern and southeastern QTP, contributing to a gradual decrease in elevation from the plateau's interior to Southeast Asia.

Our molecular dating results from a single species complex reveal, for the first time, the three-tiered landform structure of the Indo-Burma ecoregion based on botanical data. The first tier consists of the Hengduan Mountains and the Yunnan-Guizhou Plateau. The Hengduan Mountains are a series of north-south trending mountain ranges in western Sichuan and Yunnan provinces. This region encompasses several major ranges, including the Daxue Mountains, Min Mountains, and Jinsha River watershed, which originate from the southeastern margin of the QTP

(Wang et al., 2022). Elevations in this area range from 3000 to 6000 m a.s.l. with the highest peak being Kawagebo at 6740 m (Yang et al., 2022). The Hengduan Mountains are characterized by rugged terrain, steep slopes, and deep valleys dominated by alpine landscapes (Xiang et al., 2024; Chen et al., 2025). The climate is alpine with cold temperatures and heavy precipitation (Xiang et al., 2024). The Hengduan Mountains represent the first tier of the stepped topography in the Indo-Burma ecoregion, not only due to their high altitude but also because of the major rivers in this hotspot, such as the Mekong, Salween, Irrawaddy, and Red Rivers (Wen, 2017). The second tier of topography in mainland Southeast Asia is represented by the plateau region in eastern Myanmar, specifically the Shan Plateau. This area is characterized by extensive mountain ranges, high elevations, and complex terrain (Aung, 2012). The core of the third-tier terrain consists of a coastal river alluvial plain, primarily composed of three major plains and low hills interspersed among them. These include the Red River delta plain in the northeast (Larsen et al., 2017), the Ayeyarwady River downstream plain in the southwest (Chen et al., 2020), and the Mekong Delta in the south (Nguyen et al., 2000; Sakamoto et al., 2006). In a previous study, the three-tiered landform structure of mainland Southeast Asia was mainly explained from cultural and political perspectives (Wen, 2017). In contrast, our study clarifies the stepped terrain of the Indo-Burma ecoregion from a biological perspective. This research contributes to a better understanding of the topographical structure of the Indo-Burma ecoregion, its regional terrain patterns, and its evolutionary history, while positively impacting species conservation efforts.

CONCLUSIONS

Our comprehensive understanding of the evolutionary history of the *E. spicata* complex in the Indo-Burma ecoregion provides significant insights into the geological history and biogeographic structure of this region. Our data support the southeastward extrusion of Indochina along the Ailao Shan-Red River shear zone, which played a crucial role in the formation of the Truong Son Mountain Range during the Late Oligocene. Our research highlights a distinct altitudinal gradient across the Indo-Burma ecoregion, characterized by higher elevations in the north and lower areas in the south. This topographical gradient is reflected in the genetic diversity and population structure of the *E. spicata* complex, which corresponds to the tiered topography of the Indo-Burma ecoregion. Furthermore, the three-tiered landform in mainland Southeast Asia (tiered by altitude) was likely established by at least the Late Miocene, shaping the region's unique topography and influencing the evolution of its biodiversity. The tiered landscape begins with the Hengduan Mountains and the Yunnan-Guizhou Plateau as the first level, transitions to the Shan Plateau as the second level, and concludes with the coastal alluvial

plains as the third level. Our study represents a biologically informed delineation of tertiary tiered topography of the Indo-Burma ecoregion. This novel perspective offers valuable insights into the biogeographic patterns of Southeast Asia and underscores the importance of understanding the complex interplay between geological events and biological diversity.

AUTHOR CONTRIBUTIONS

C.Y.Z.: conceptualization, investigation, writing original draft, review, editing, visualization. G.L.C.: investigation, review, editing, visualization. J.L.H., P.H.H., M.L., R.P.S., O.Y.F., X.C., Y.G.S., G.X.H., K.Q.X.: review, editing. L.L. and S.S.Z.: investigation, resources. Y.H.T.: writing original draft, investigation, resources. H.H.M.: conceptualization, investigation, resources, writing original draft, review, editing, visualization, funding acquisition, and supervision. J.L.: conceptualization, supervision.

ACKNOWLEDGMENTS

We sincerely thank the editors and two anonymous reviewers for their constructive feedback that significantly improved this manuscript. Special gratitude is extended to Qiu-Yue Zhang, Han-Yang Lin, Jian-Hua Xiao, Chao-Nan Cai, and Zhi-Fang Liu for assistance with data collection and analysis. This work was supported by the Natural Science Foundation of Yunnan Province, China (No. 202301AU070145); National Natural Science Foundation of China (No. 42171063); Southeast Asia Biodiversity Research Institute, Chinese Academy of Sciences (No. Y4ZK111B01); the Yunnan Revitalization Talent Support Program in Yunnan Province (XDYC-QNRC-2022-0028); Yunnan Revitalization Talent Support Program Innovation Team Project (202405AS350019); the CAS Light of West China Program; and the 14th Five-Year Plan of the Xishuangbanna Tropical Botanical Garden, Chinese Academy of Sciences (XTBG-1450101).

DATA AVAILABILITY STATEMENT

All data required to replicate the results are included in the Supporting Information files. Haplotype sequences are deposited in GenBank as accessions PQ142373–PQ142622 and ribotype sequences as PQ154494–PQ154524. The original data sets are available via FigShare at <https://doi.org/10.6084/m9.figshare.29069411>.

ORCID

Hong-Hu Meng  <https://orcid.org/0000-0002-4504-0001>

Jie Li  <https://orcid.org/0000-0001-8067-749X>

REFERENCES

- Álvarez, I., and J. F. Wendel. 2003. Ribosomal ITS sequences and plant phylogenetic inference. *Molecular Phylogenetics and Evolution* 29: 417–434.
- Aung, A. K. 2012. The Paleozoic stratigraphy of Shan Plateau, Myanmar, an updated version. *Journal of the Myanmar Geoscience Society* 5: 1–73.
- Baele, G., W. L. S. Li, A. J. Drummond, M. A. Suchard, and P. Lemey. 2013. Accurate model selection of relaxed molecular clocks in Bayesian phylogenetics. *Molecular Biology and Evolution* 30: 239–243.
- Bandelt, H. J., P. Forster, and A. Röhl. 1999. Median-joining networks for inferring intraspecific phylogenies. *Molecular Biology and Evolution* 16: 37–48.
- Barreda, V. D., M. C. Zamalao, M. A. Gandolfo, C. Jaramillo, and P. Wilf. 2020. Early Eocene spore and pollen assemblages from the Laguna del Hunco fossil lake beds, Patagonia, Argentina. *International Journal of Plant Sciences* 181: 594–615.
- Bossuyt, F., and M. C. Milinkovitch. 2001. Amphibians as indicators of early tertiary “Out-of-India” dispersal of vertebrates. *Science* 292: 93–95.
- Che, J., W. W. Zhou, J. S. Hu, F. Yan, T. J. Papenfuss, D. B. Wake, and Y. P. Zhang. 2010. Spiny frogs (*Paini*) illuminate the history of the Himalayan region and Southeast Asia. *Proceedings of the National Academy of Sciences, USA* 107: 13765–13770.
- Chen, C. H., Y. Bai, X. M. Fang, Q. Xu, T. Zhang, T. Deng, J. K. He, and Q. H. Chen. 2020. Lower-altitude of the Himalayas before the mid-Pliocene as constrained by hydrological and thermal conditions. *Earth and Planetary Science Letters* 545: 116422.
- Chen, Y., Y. Chen, X. Hu, and J. Feng. 2025. Characterizing pattern of topography and geomorphology in the Hengduan Mountains, Southwest China. *Journal of Environmental & Earth Sciences* 7: 414–422.
- Clark, M. K., L. M. Schoenbohm, L. H. Royden, K. X. Whipple, B. C. Burchfiel, X. Zhang, W. Tang, et al. 2005. Surface uplift, tectonics, and erosion of eastern Tibet from large-scale drainage patterns. *Tectonics* 23: TC1006.
- da Silva, P.H.M. and O. S. Abrahão. 2021. Gene flow and spontaneous seedling establishment around genetically modified eucalypt plantations. *New Forests* 52: 349–361.
- Dilcher, D. L., F. W. Potter, and W. L. Crepet. 1976. Investigations of angiosperms from the Eocene of North America: juglandaceous winged fruits. *American Journal of Botany* 63: 532–544.
- Ding, L., P. Kapp, F. L. Cai, C. N. Garzione, Z. Y. Xiong, H. Q. Wang, and C. Wang. 2022. Timing and mechanisms of Tibetan Plateau uplift. *Nature Reviews Earth & Environment* 3: 652–667.
- Drummond, A. J., and A. Rambaut. 2007. BEAST: Bayesian evolutionary analysis by sampling trees. *BMC Evolutionary Biology* 7: 214.
- Emadzade, K., and E. Hörandl. 2011. Northern Hemisphere origin, transoceanic dispersal, and diversification of Ranunculaceae DC. (Ranunculaceae) in the Cenozoic. *Journal of Biogeography* 38: 517–530.
- Excoffier, L., G. Laval, and S. Schneider. 2007. Arlequin (version 3.0): an integrated software package for population genetics data analysis. *Evolutionary Bioinformatics Online* 1: 47–50.
- Excoffier, L., P. E. Smouse, and J. M. Quattro. 1992. Analysis of molecular variance inferred from metric distances among DNA haplotypes: application to human mitochondrial DNA restriction data. *Genetics* 131: 479–491.
- Fanget, A. S., L. Loncke, F. Pattier, T. Marsset, W. R. Roest, C. Talloire, X. Durrieu de Madron, and F. J. Hernández-Molina. 2020. A synthesis of the sedimentary evolution of the Demerara Plateau (Central Atlantic Ocean) from the late Albian to the Holocene. *Marine and Petroleum Geology* 114: 104195.
- Feng, J., H. Yao, L. Chen, and W. Wang. 2021. Massive lithospheric delamination in southeastern Tibet facilitating continental extrusion. *National Science Review* 9: nwab174.
- Fick, S. E., and R. J. Hijmans. 2017. WorldClim 2: new 1-km spatial resolution climate surfaces for global land areas. *International Journal of Climatology* 37: 4302–4315.
- Fu, Y. X. 1997. Statistical tests of neutrality of mutations against population growth, hitchhiking and background selection. *Genetics* 147: 915–925.
- Fu, Y. X., and W. H. Li. 1993. Statistical tests of neutrality of mutations. *Genetics* 133: 693–709.
- Garcés, M., M. López-Blanco, L. Valero, E. Beamud, J. A. Muñoz, B. Oliva-Urcia, A. Vinyoles, et al. 2020. Paleogeographic and sedimentary evolution of the South Pyrenean foreland basin. *Marine and Petroleum Geology* 113: 104105.

- Gower, D. J., A. Kupfer, O. V. Oommen, W. Himstedt, R. A. Nussbaum, S. P. Loader, B. Presswell, et al. 2002. A molecular phylogeny of ichthyophiid caecilians (Amphibia: Gymnophiona: Ichthyophiidae): out of India or out of South East Asia? *Proceedings of the Royal Society, B, Biological Sciences* 269: 1563–1569.
- Grafen, A. 1989. The phylogenetic regression. *Philosophical Transactions of the Royal Society, B, Biological Sciences* 326: 119–157.
- Harpending, H. C. 1994. Signature of ancient population growth in a low-resolution mitochondrial DNA mismatch distribution. *Human Biology* 66: 591–600.
- Hedrn, M., and R. Lorenz. 2019. Seed dispersal and fine-scale genetic structuring in the asexual *Nigritella miniata* (Orchidaceae) in the Alps. *Botanical Journal of the Linnean Society* 190: 83–100.
- Hermesen, E. J., and M. A. Gandolfo. 2016. Fruits of Juglandaceae from the Eocene of South America. *Systematic Botany* 41: 316–328.
- Herrera-Alsina, L., A. C. Algar, G. Bocedi, C. Gubry-Rangin, L. T. Lancaster, P. Mynard, O. G. Osborne, et al. 2021. Ancient geological dynamics impact neutral biodiversity accumulation and are detectable in phylogenetic reconstructions. *Global Ecology and Biogeography* 30: 1633–1642.
- Hijmans, R. J. 2020. raster: Geographic data analysis and modeling. R package version 3.1–5. Website: <https://cran.r-project.org/package=raster>
- Ho, S. Y. W., and M. J. Phillips. 2009. Accounting for calibration uncertainty in phylogenetic estimation. *Molecular Biology and Evolution* 26: 2525–2533.
- Huang, J. F., S. Q. Li, R. Xu, and Y. Q. Peng. 2023. East-West genetic differentiation across the Indo–Burma hotspot: evidence from two closely related dioecious figs. *BMC Plant Biology* 23: 321.
- Huang, P. H., T. R. Wang, M. Li, Z. J. Lu, R. P. Su, O. Y. Fang, L. Li, et al. 2024. RAD-seq data for *Engelhardia roxburghiana* provide insights into the palaeogeography of Hainan Island and its relationship to mainland China since the late Eocene. *Palaeogeography, Palaeoclimatology, Palaeoecology* 651: 112392.
- Huang, P. H., Y. G. Song, J. Li and H. H. Meng. 2025. Did Hainan Island (Southern China) undergo significant cenozoic tectonic displacement, and impact its biota's sourcing and evolution? *Journal of Biogeography* 52: e15168.
- Huelsenbeck, J. P., and F. Ronquist. 2001. MRBAYES: Bayesian inference of phylogenetic trees. *Bioinformatics* 17: 754–755.
- Janssens, S. B., F. Vandelook, E. De Langhe, B. Verstraete, E. Smets, I. Vandenhouwe, and R. Swennen. 2016. Evolutionary dynamics and biogeography of Musaceae reveal a correlation between the diversification of the banana family and the geological and climatic history of Southeast Asia. *New Phytologist* 210: 1453–1465.
- Kass, R. E., and A. E. Raftery. 1995. Bayes factors. *Journal of the American Statistical Association* 90: 773–795.
- Kooyman, R. M., R. J. Morley, D. M. Crayn, E. M. Joyce, M. Rossetto, J. W. F. Slik, J. S. Strijk, et al. 2019. Origins and assembly of Malesian rainforests. *Annual Review of Ecology, Evolution, and Systematics* 50: 119–143.
- Kotlínek, M., T. Těšitelová, J. Košnar, P. Fibich, L. Hemrová, P. Koutecký, Z. Münzbergová, and J. Jersáková. 2020. Seed dispersal and realized gene flow of two forest orchids in a fragmented landscape. *Journal of Plant Biology* 22: 522–532.
- Lai, Y. J., J. Wen, Z. K. Zhou, S. Ge, R. A. Spicer, Z. D. Chen, and Y. Y. Chen. 2025a. Uplift history and biological evolution of the Himalaya. *Journal of Systematics and Evolution* 63: 1–4.
- Lai, Y. J., J. F. Ye, B. Liu, Y. Liu, A. M. Lu, F. W. Wei, and Z. D. Chen. 2025b. Integrating fossil and extant plant communities to calibrate paleoelevation of Qinghai-Tibet Plateau. *Journal of Systematics and Evolution* 63: 25–38.
- Larsen, F., L. V. Tran, H. Van Hoang, L. T. Tran, A. V. Christiansen, and N. Q. Pham. 2017. Groundwater salinity influenced by Holocene seawater trapped in incised valleys in the Red River delta plain. *Nature Geoscience* 10: 376–381.
- Lee, J. S. 1939. The geology of China. Thomas Murby Press, London, UK.
- Leloup, P. H., N. Arnaud, R. Lacassin, J. R. Kienast, T. M. Harrison, T. T. P. Trong, A. Replumaz, and P. Tapponnier. 2001. New constraints on the structure, thermochronology, and timing of the Ailao Shan-Red River shear zone, SE Asia. *Journal of Geophysical Research: Solid Earth* 106: 6683–6732.
- Li, S. H., T. Su, R. A. Spicer, C. L. Xu, S. Sherlock, A. Halton, G. Hoke, et al. 2020. Oligocene deformation of the Chuandian Terrane in the SE Margin of the Tibetan Plateau related to the westward extrusion of Indochina. *Tectonics* 39: e2019TC005974.
- Li, X. Q., H. W. Peng, K. L. Xiang, X. G. Xiang, F. Jabbour, R. D. C. Ortiz, P. S. Soltis, et al. 2024. Phylogenetic evidence clarifies the history of the extrusion of Indochina. *Proceedings of the National Academy of Sciences, USA* 121: e2322527121.
- Liu, J. L., Y. Tang, M. D. Tran, S. Y. Cao, L. Zhao, Z. C. Zhang, Z. D. Zhao, and W. Chen. 2012. The nature of the Ailao Shan-Red River (ASRR) shear zone: Constraints from structural, microstructural and fabric analyses of metamorphic rocks from the Diancang Shan, Ailao Shan and Day Nui Con Voi massifs. *Journal of Asian Earth Sciences* 47: 231–251.
- Lu, A. M., D. E. Stone, and L. J. Grauke. 1999. Juglandaceae. Flora of China, 278–280. Science Press, Beijing, China; Missouri Botanical Garden Press, St. Louis, MO, USA.
- Luo, A. B., J. J. Fan, B. C. Zhang, and Y. J. Hao. 2022. Cretaceous uplift history of the Tibetan Plateau: insights from the transition of marine to terrestrial facies in central Tibet. *Palaeogeography, Palaeoclimatology, Palaeoecology* 601: 111103.
- Luo, Y. F., and S. Q. Li. 2018. Cave Stedocys spitting spiders illuminate the history of the Himalayas and Southeast Asia. *Ecography* 41: 414–423.
- Maddison, W. P., and D. R. Maddison. 2019. Mesquite: A modular system for evolutionary analysis. Version 3.61. Website: <http://mesquiteproject.org>
- Maneerat, P., and R. Bürgmann. 2022. Geomorphic expressions of active tectonics across the Indo-Burma Range. *Journal of Asian Earth Sciences* 223: 105008.
- Manning, W. E. 1966. New combinations and notes on *Engelhardia* (Juglandaceae) of the Old World. *Bulletin of the Torrey Botanical Club* 93: 34–52.
- Manos, P. S., P. S. Soltis, D. E. Soltis, S. R. Manchester, S. H. Oh, C. D. Bell, D. L. Dilcher, and D. E. Stone. 2007. Phylogeny of extant and fossil Juglandaceae inferred from the integration of molecular and morphological data sets. *Systematic Biology* 56: 412–430.
- Manos, P. S., and D. E. Stone. 2001. Evolution, phylogeny, and systematics of the Juglandaceae. *Annals of the Missouri Botanical Garden* 88: 231–269.
- Mao, K. S., Y. Wang, and J. Q. Liu. 2021. Evolutionary origin of species diversity on the Qinghai-Tibet Plateau. *Journal of Systematics and Evolution* 59: 1142–1158.
- Martins, E. P., and T. F. Hansen. 1997. Phylogenies and the comparative method: A general approach to incorporating phylogenetic information into the analysis of interspecific data. *American Naturalist* 149: 646–667.
- Matzke, N. J. 2013. Probabilistic historical biogeography: New models for founder-event speciation, imperfect detection, and fossils allow improved accuracy and model-testing. *Frontiers in Biogeography* 5: 1–16.
- Meng, H. H., and Y. G. Song. 2023. Biogeographic patterns in Southeast Asia: Retrospectives and perspectives. *Biodiversity Science* 31: 23261.
- Meng, H. H., Y. G. Song, G. X. Hu, et al. 2025. Evolution of East Asian subtropical evergreen broad-leaved forests: When and how? *Journal of Systematics and Evolution*. <https://doi.org/10.1111/jse.70001>
- Meng, H. H., T. Su, Y. J. Huang, H. Zhu, and Z. K. Zhou. 2015. Late Miocene *Palaeocarya* (Engelhardiaceae: Juglandaceae) from Southwest China and its biogeographic implications. *Journal of Systematics and Evolution* 53: 499–511.
- Meng, H. H., C. Y. Zhang, S. L. Low, L. Li, J. Y. Shen, Nurainas, and Y. Zhang. 2022a. Two new species from Sulawesi and Borneo facilitate phylogeny and taxonomic revision of *Engelhardia* (Juglandaceae). *Plant Diversity* 44: 552–564.
- Meng, H. H., C. Y. Zhang, Y. G. Song, X. Yu, G. L. Cao, L. Li, C. N. Cai, et al. 2022b. Opening a door to the spatiotemporal history of plants from the tropical Indochina Peninsula to subtropical China. *Molecular Phylogenetics and Evolution* 171: 107458.

- Minh, B. Q., H. A. Schmidt, O. Chernomor, D. Schrempf, M. D. Woodhams, A. von Haeseler, and R. Lanfear. 2020. IQ-TREE 2: new models and efficient methods for phylogenetic inference in the genomic era. *Molecular Biology and Evolution* 37: 1530–1534.
- Mittermeier, R. A., N. Myers, and C. G. Mittermeier. 2002. Hotspots: Earth's biologically richest and most endangered terrestrial ecoregions. *Journal of Mammalogy* 83: 630–633.
- Mittermeier, R. A., P. Robles-Gil, M. Hoffmann, J. Pilgrim, T. Brooks, C. G. Mittermeier, J. L. Lamoreux, and G. A. B. Fonseca. 2005. Hotspots revisited: Earth's biologically richest and most endangered terrestrial ecoregions. Conservation International, Washington, D.C., USA.
- Myers, N., R. A. Mittermeier, C. G. Mittermeier, G. A. Da Fonseca, and J. Kent. 2000. Biodiversity hotspots for conservation priorities. *Nature* 403: 853–858.
- Nguyen, V. L., T. K. O. Ta, and M. Tateishi. 2000. Late Holocene depositional environments and coastal evolution of the Mekong River Delta, Southern Vietnam. *Journal of Asian Earth Sciences* 18: 427–439.
- Nylander, J. 2004. MrModeltest V2. program distributed by the author. *Bioinformatics* 24: 581–583.
- Paradis, E., J. Claude, and K. Strimmer. 2004. APE: analyses of phylogenetics and evolution in R language. *Bioinformatics* 20: 289–290.
- Rambaut, A. 2018. FigTree v.1.4.4. Website: <http://tree.bio.ed.ac.uk/software/figtree/>
- Rambaut, A., M. A. Suchard, D. Xie, D. Xie, and A. J. Drummond. 2014. Tracer version 1.6. Website: <http://tree.bio.ed.ac.uk/software/tracer/>
- Ree, R. H., and S. A. Smith. 2008. Maximum likelihood inference of geographic range evolution by dispersal, local extinction, and cladogenesis. *Systematic Biology* 57: 4–14.
- Rozas, J., A. Ferrer-Mata, J. C. Sánchez-DelBarrio, S. Guirao-Rico, P. Librado, S. E. Ramos-Onsins, and A. Sánchez-Gracia. 2017. DnaSP 6: DNA sequence polymorphism analysis of large data sets. *Molecular Biology and Evolution* 34: 3299–3302.
- Sakamoto, T., N. Van Nguyen, H. Ohno, N. Ishitsuka, and M. Yokozawa. 2006. Spatio-temporal distribution of rice phenology and cropping systems in the Mekong Delta with special reference to the seasonal water flow of the Mekong and Bassac rivers. *Remote Sensing of Environment* 100: 1–16.
- Sauquet, H., S. Y. W. Ho, M. A. Gandolfo, G. J. Jordan, P. Wilf, D. J. Cantrill, M. J. Bayly, et al. 2012. Testing the impact of calibration on molecular divergence times using a fossil-rich group: the case of *Nothofagus* (Fagales). *Systematic Biology* 61: 289–313.
- Schärer, U., Z. Lian-Sheng, and P. Tapponnier. 1994. Duration of strike-slip movements in large shear zones: The Red River belt, China. *Earth and Planetary Science Letters* 126: 379–397.
- Song, Y. G., Y. Fragnière, H. H. Meng, Y. Li, B. Sébastien, A. Corrales, S. Manchester, et al. 2020. Global biogeographic synthesis and priority conservation regions of the relict tree family Juglandaceae. *Journal of Biogeography* 47: 643–657.
- Swofford, D. L. 2002. PAUP*: phylogenetic analysis using parsimony (*and other methods), version 4.0b10. Sinauer, Sunderland, MA, USA.
- Tajima, F. V. 1989. Statistical method for testing the neutral mutation hypothesis by DNA polymorphism. *Genetics* 123: 585–595.
- van Dijk, P. P., P. Ashton, and J. Ma. 1999. Indo-Burma. In R. A. Mittermeier, N. Myers, and C. G. Mittermeier [eds.], Hotspots: Earth's biologically richest and most endangered terrestrial ecoregions. Sierra Madre Press, Mexico City, Mexico.
- van Hinsbergen, D. J. J., P. C. Lippert, G. Dupont-Nivet, N. McQuarrie, P. V. Doubrovine, W. Spakman, and T. H. Torsvik. 2012. Greater India Basin hypothesis and a two-stage Cenozoic collision between India and Asia. *Proceedings of the National Academy of Sciences, USA* 109: 7659–7664.
- Wang, E. Q. 2017. Discussion on the initial collision time between India and the Eurasian Continent. *Science China (Earth Sciences)* 47: 284–292.
- Wang, X. Y., D. Liang, X. M. Wang, M. K. Tang, Y. Liu, S. Y. Liu, and P. Zhang. 2022. Phylogenomics reveals the evolution, biogeography, and diversification history of voles in the Hengduan Mountains. *Communications Biology* 5: 1124.
- Wen, J. X. 2017. Who is at the center of the world? CITIC Press, Beijing, China.
- Wilf, P. 2012. Rainforest conifers of Eocene Patagonia: attached cones and foliage of the extant Southeast Asian and Australasian genus *Dacrycarpus* (Podocarpaceae). *American Journal of Botany* 99:562–584.
- Woodruff, D. S. 2010. Biogeography and conservation in Southeast Asia: how 2.7 million years of repeated environmental fluctuations affect today's patterns and the future of the remaining refugial-phase biodiversity. *Biodiversity and Conservation* 19: 919–941.
- Wu, Y. H., F. Yan, B. L. Stuart, E. Prendini, C. Suwannapoom, H. A. Dahn, B. L. Zhang, et al. 2020. A combined approach of mitochondrial DNA and anchored nuclear phylogenomics sheds light on unrecognized diversity, phylogeny, and historical biogeography of the torrent frogs, genus *Amolops* (Anura: Ranidae). *Molecular Phylogenetics and Evolution* 148: 106789.
- Xiang, K. L., A. S. Erst, J. Yang, H. W. Peng, R. D. C. Ortiz, F. Jabbour, T. V. Erst, and W. Wang. 2021. Biogeographic diversification of *Eranthis* (Ranunculaceae) reflects the geological history of the three great Asian plateaus. *Proceedings of the Royal Society, B, Biological Sciences* 288: 20210281.
- Xiang, R., C. R. Steger, S. Li, L. Pellissier, S. L. Sørland, S. D. Willett, and C. Schär. 2024. Assessing the regional climate response to different Hengduan Mountains geometries with a high resolution regional climate model. *Journal of Geophysical Research: Atmospheres* 129: e2023JD040208.
- Yang, Z., W. Xi, Z. Yang, Z. Shi, and T. Qian. 2022. Monitoring and prediction of glacier deformation in the Meili Snow Mountain based on InSAR technology and GA-BP neural network algorithm. *Sensors* 22: 8350.
- Yin, A., and T. M. Harrison. 2000. Geologic evolution of the Himalayan-Tibetan orogen. *Annual Review of Earth and Planetary Sciences* 28: 211–280.
- Yu, Y., A. J. Harris, C. Blair, and X. He. 2015. RASP (Reconstruct Ancestral State in Phylogenies): A tool for historical biogeography. *Molecular Phylogenetics and Evolution* 87: 46–49.
- Zhang, C. Y., S. Ling Low, Y. G. Song, Nurainas, G. Kozłowski, L. Li, S. S. Zhou, et al. 2020. Shining a light on species delimitation in the tree genus *Engelhardia* Leschenault ex Blume (Juglandaceae). *Molecular Phylogenetics and Evolution* 152: 106918.
- Zhang, J. B., R. Q. Li, X. G. Xiang, S. R. Manchester, L. Lin, W. Wang, J. Wen, and Z. D. Chen. 2013. Integrated fossil and molecular data reveal the biogeographic diversification of the eastern Asian–eastern north American disjunct hickory genus (*Carya* Nutt.). *PLoS One* 8: e70449.
- Zhang, L., Z. L. Liang, X. P. Fan, N. T. Lu, X. M. Zhou, H. J. Wei and L.-B. Zhang. 2024. The Indo-Burma biodiversity hotspot for ferns: updated phylogeny, hidden diversity, and biogeography of the java fern genus *Leptochilus* (Polypodiaceae). *Plant Diversity*, 46: 698–712.
- Zhang, L. G., X. Q. Li, W. T. Jin, Y. J. Liu, Y. Zhao, J. Rong and X. G. Xiang. 2023. Asymmetric migration dynamics of the tropical Asian and Australasian floras. *Plant Diversity* 45: 20–26.
- Zhang, M. H., Z. L. Nie, R. A. Fairbanks, J. Liu, R. Litterman, G. Johnson, S. Handy, and J. Wen. 2025. Phylogenomic insights into species relationships, reticulate evolution, and biogeographic diversification of the ginseng genus *Panax* (Araliaceae), with an emphasis on the diversification in the Himalaya-Hengduan Mountains. *Journal of Systematics and Evolutions* 63: 99–114.
- Zhang, X. H., Z. L. Wang, F. H. Hou, J. Y. Yang, and X. W. Guo. 2014. Terrain evolution of China seas and land since the Indo-China movement and characteristics of the stepped landform. *Chinese Journal of Geophysics* 57: 3968–3980 [in Chinese].
- Zhang, Z. M., X. Dong, M. Santosh, F. Liu, W. Wang, F. Yiu, Z. Y. He, and K. Shen. 2012. Petrology and geochronology of the Namche Barwa Complex in the eastern Himalayan syntaxis, Tibet: constraints on the origin and evolution of the north-eastern margin of the Indian Craton. *Gondwana Research* 21: 123–137.
- Zhao, J. L., Y. M. Xia, C. H. Cannon, W. J. Kress, and Q. J. Li. 2016. Evolutionary diversification of alpine ginger reflects the early uplift of the Himalayan–Tibetan Plateau and rapid extrusion of Indochina. *Gondwana Research* 32: 232–241.

SUPPORTING INFORMATION

Additional supporting information can be found online in the Supporting Information section at the end of this article.

Appendix S1. Supplementary figures and tables.

Figure S1. Distribution of the number of pairwise nucleotide differences for ITS and plastid DNA of the *E. spicata* complex.

Figure S2. Phylogenies inferred using maximum likelihood (ML) and Bayesian inference (BI) based on the combined plastid DNA haplotypes.

Figure S3. Phylogenies inferred using maximum likelihood (ML) and Bayesian inference (BI) based on nuclear ITS data.

Figure S4. Bayesian divergence time estimates of the *Engelhardia* species based on the ITS data set.

Figure S5. Ancestral range reconstruction using BioGeoBEARS and the DEC model.

Figure S6. Networks of the *E. spicata* complex from plastid DNA; each circle indicates a single haplotype drawn in proportion to its frequency.

Figure S7. Ancestral reconstruction utilizing the squared-change parsimony method (mapped on the plastid phylogeny), phylogenetic independent contrast (PIC) method and phylogenetic generalized least squares (PGLS) method analyses; the mean elevation and 95% confidence interval boundaries are noted.

Table S1. Details of *E. spicata* complex populations used in molecular analysis, sample size (*N*), and plastid DNA haplotypes (*H*) observed.

Table S2. Primers for the amplification of DNA regions in various populations of *E. spicata* complex.

Table S3. Comparison of four clock models in BEAST analyses via Bayes factors.

Table S4. Comparison of two tree prior processes in BEAST analyses via Bayes factors.

Table S5. Comparison of the fit of six models of biogeographical range evolution and model-specific estimates for different parameters.

Table S6. Summary of biogeographic stochastic map (BSM) from the DEC model.

Table S7. Distribution records used for species elevation analysis.

Table S8. Analysis of molecular variance (AMOVA) for plastid DNA data and ITS from three regions and all regions.

Table S9. Molecular diversity indices and neutral tests from three biogeographic regions and all biogeographic regions.

Table S10. Analysis of elevation variance (ANOVA) for the *E. spicata* complex across the three regions.

How to cite this article: Zhang, C.-Y., G.-L. Cao, J.-L. Hu, P.-H. Huang, M. Li, R.-P. Su, O.-Y. Fang, et al. 2025. The reconstructed evolutionary history of the *Engelhardia spicata* complex highlights the impact of a three-tiered landform in the Indo-Burma ecoregion. *American Journal of Botany* 112(8): e70077. <https://doi.org/10.1002/ajb2.70077>